J. Fluid Mech. (1975), *vol.* 72, *part* 4, *pp.* 673–694
Printed in Great Britain

On higher-order spectra of turbulence

By C. W. VAN ATTA
Scripps Institution of Oceanography, University of California, La Jolla
AND J. C. WYNGAARD
Air Force Cambridge Research Laboratories, Bedford, Massachusetts 01731†

(Received 21 January 1975 and in revised form 3 June 1975)

Measurements of higher-order spectra of turbulent velocity fluctuations in the atmospheric boundary layer over the open ocean and land produce the interesting result that, in the wavenumber range designated originally by Kolmogorov as an inertial subrange, the functional dependence of the spectra on wavenumber is practically independent of the order of the spectrum. These results confirm the observation of Dutton & Deaven that their extension by a dimensional similarity argument of the original Kolmogorov theory to higher-order spectra was not valid. In the present work, we derive an alternative generalization of the Kolmogorov ideas for spectra of arbitrary order. The results of this generalization describe the dependence upon wavenumber of the available data quite well. We also present theoretical calculations based on a Gaussian model for the fluctuating velocity field which furnish quantitative predictions for spectra of arbitrary order that are also in good agreement with the measurements, both in functional form and in absolute value.

Comparison of results based on the Gaussian model with laboratory measurements obtained in a free shear layer shows that the Gaussian theory predicts accurately all the available normalized higher-order spectra for all frequencies. When the corresponding measured higher-order moments are close to those expected for a Gaussian process, the Gaussian theory also correctly predicts the absolute magnitudes of the higher-order spectra.

1. Introduction

Interest in measurements of higher-order statistical functions of turbulent velocity fluctuations in fluid turbulence is partially based on the hope that their determination will provide crucial tests of theories which differ little for lower-order quantities, but which provide wildly conflicting results for higher-order functions. The simplest and most extensive theoretical predictions available are for turbulence in flows with very large values of the Reynolds number. The largest Reynolds numbers achieved in experiments have been obtained in flows of geophysical interest in the atmosphere and oceans.

A great number of measurements of energy spectra (the lowest-order spectral statistic) have been made, but only recently has interest arisen in higher-order

† Present address: Wave Propagation Laboratory, N.O.A.A., Boulder, Colorado 80302.

spectra, of squares and higher powers of fluctuating turbulent variables. There has been considerable interest in such spectra in statistical communication problems for some time, however.

The term 'higher-order spectra' has been previously used in several different ways in the turbulence literature. In the present work it has the same meaning as in the atmospheric work of Dutton & Deaven (1972) and in the laboratory study of Champagne, Pao & Wygnanski (1976). Here the nth-order spectrum is defined as the power spectrum of the nth power of the fluctuating velocity. This definition differs from another one in common use, namely that the order of the spectrum denotes the number of frequency or wavenumber variables of which the spectrum is a function, and also the dimension of the corresponding displacement vector in its Fourier transform, the $(n+1)$th-order correlation. General characteristics of such polyspectra have been described in detail by Brillinger & Rosenblatt (1967). These include bispectra, which are functions of two frequency variables, trispectra, which are functions of three frequency variables, etc. In the present work, we are not concerned with this latter type of higher-order spectrum, and shall be dealing only with power spectra of powers of the fluctuating velocity.

Dutton & Deaven (1972) considered the behaviour of spectra of algebraic powers of the velocity fluctuations of up to fourth order. Defining $\phi_n(k)$ to be such that $\phi_n(k)\,dk$ is the spectral contribution to $\langle u^{2n}\rangle$ from the wavenumber interval k to $k+dk$ we have

$$\langle (u^n - \langle u^n\rangle)^2\rangle = \langle u^{2n}\rangle - \langle u^n\rangle^2 \equiv \int_{-\infty}^{\infty} \phi_n(k)\,dk. \tag{1}$$

In analogy with Kolmogorov's (1941) development of the second-order structure function and corresponding spectrum ϕ_1, Dutton & Deaven argued that for large Reynolds numbers an inertial subrange of wavenumbers might exist in which all $\phi_n(k)$ depend only upon the wavenumber k and the mean rate ϵ of dissipation of turbulent kinetic energy per unit mass.

Assuming, in analogy with Kolmogorov's original inertial-subrange analysis (which results in $\phi_1(k) = \alpha\epsilon^{\frac{2}{3}}k^{-\frac{5}{3}}$), that $\phi_n(k) = \alpha_n \epsilon^{\gamma} k^{\lambda}$, dimensional analysis yields $\gamma = \frac{2}{3}n$, $\lambda = -\frac{1}{3}(2n+3)$ and

$$\phi_1 \sim k^{-\frac{5}{3}}, \quad \phi_2 \sim k^{-\frac{7}{3}}, \quad \phi_3 \sim k^{-3}, \quad \phi_4 \sim k^{-\frac{11}{3}}, \quad \text{etc.} \tag{2}$$

Dutton & Deaven computed higher-order spectra of up to fourth order ($n = 4$) for all three velocity components from samples of atmospheric turbulence obtained at four different altitudes with instrumented aircraft. The lower-altitude data (250 and 750 ft), obtained over the Kansas plains, were considered as examples of boundary-layer turbulence, while the higher-altitude data (60 000 and 30 000 ft) were characteristic of clear-air turbulence (CAT) over the Sierra Nevada and severe CAT near Grand Junction, Colorado, respectively. The behaviour for $n \geqslant 2$ described by (2) was not observed in any of these cases. As shown in the example of their data replotted in figure 5, rather than increasing in slope with increasing order for the higher frequency range, the higher-order spectra either retained an approximately $-\frac{5}{3}$-power law or decreased somewhat in slope. This behaviour led Dutton & Deaven to conjecture that "it is clear that the $-\frac{5}{3}$ power law generally observed in atmospheric turbulence in the range 100 to 1000 m does not indicate an inertial range in which spectral properties [of higher-order spectra] depend only on $\langle\epsilon\rangle$ and k". This conjecture served as the basic stimulus for the present investigation. If the analysis leading to (2) were correct, it would appear to weaken the foundations of Kolmogorov's inertial-subrange theory sufficiently to require a complete reassessment of the underlying concepts of an energy cascade as first proposed by Richardson (1920).

In the present paper, we propose an alternative extension of Kolmogorov's ideas, which describes the available data quite well. The key factor in the present dimensional argument is an order-dependent dissipation term ϵ_n, which appears in the dynamical equation for $\langle u^{2n}\rangle$.

As noted by Dutton & Deaven, the probability density of the velocity fluctuations in atmospheric turbulence is generally not even approximately Gaussian. In clear-air turbulence, there are clearly more large gusts and more nearly zero values than would be expected if the density were Gaussian. The lower-altitude boundary-layer data appear to fit a Gaussian distribution much more closely. One knows that the distribution cannot, in principle, be exactly Gaussian. If it were, the probability densities of velocity derivatives would also necessarily be Gaussian, in direct conflict with an extensive body of experimental and theoretical evidence. The grid-turbulence measurements of Townsend (1947) furnish an example of a velocity field for which the one-point density $p(u)$ is very nearly Gaussian, but for which the density $p(\partial u/\partial t)$ of its derivative is clearly non-Gaussian. Later work by Frenkiel & Klebanoff (1967) and by Van Atta & Chen (1968) showed that for grid turbulence a Gaussian distribution could be used to predict even-order single- and multi-point moments of the velocity field to very high order with only a small error. The Gaussian assumption is thus a good approximation for the calculation of certain statistical properties of the velocity field, like even-order moments of the velocity, while it is not a good approximation for other properties, like velocity derivatives. It is of course also of no use whatever for multi-point odd-order moments (e.g. triple correlations), which are all identically zero for a multivariate Gaussian distribution.

Champagne *et al.* (1976) used measurements of higher-order spectra ($n \leqslant 4$) in a turbulent mixing layer to determine the contributions of various frequencies to higher moments of the velocity fluctuations. There was relatively little evidence of inertial-subrange behaviour in their ϕ_1 spectra, but they noted that, in the approximately $k^{-\frac{5}{3}}$ region of their first-order energy spectrum, the higher-order spectra did not follow the behaviour predicted by (2), but became somewhat less steep with increasing order.

The question naturally arises as to whether the Gaussian assumption for the probability density of the velocity fluctuations leads to realistic predictions for higher-order spectra of the velocity, and how these would compare with measured spectra and those predicted from the extended Kolmogorov arguments. In the present work we shall see that in the inertial subrange the Gaussian assumption produces results for higher-order spectra that are in excellent agreement with the experiments of Dutton & Deaven and with some new spectral measurements obtained in the atmospheric boundary layer over the open ocean. Comparison with some lower Reynolds number laboratory data of

Champagne *et al.* (1976) shows that the results of the Gaussian calculations are in close absolute agreement with the measured results when the measured higher-order moments are close to the values expected for a Gaussian distribution.

2. Theory

In this section, we present two distinct theoretical attempts to determine the form of higher-order spectra in the inertial subrange. The first is a dimensional argument which can predict only the functional variation with wavenumber or frequency of higher-order spectra. The second analysis, based on an assumption of Gaussianity, predicts the same wavenumber variation, but has the distinct advantage of yielding quantitative predictions for the spectral levels.

2.1. *The maintenance of* $\langle u^{2n}\rangle$ *and implications for higher-order spectra*

The conservation equations which identify the mechanisms which maintain higher moments in turbulence follow directly from the Navier–Stokes equation. We shall show that these moment equations also suggest which parameters govern the inertial-range behaviour of higher-order spectra.

We start from

$$\partial\langle u_\alpha^{2n}\rangle/\partial t = 2n\langle u_\alpha^{2n-1}\,\partial u_\alpha/\partial t\rangle, \tag{3}$$

where $\mathbf{u} = (u, v, w)$ is the turbulent velocity vector. An equation for the right side of (3) can be derived from the $\partial u_\alpha/\partial t$ equation:

$$u_{\alpha,t} + U_{\alpha,j}u_j + u_{\alpha,j}U_j + u_{\alpha,j}u_j - \langle u_{\alpha,j}u_j\rangle = -p_{,\alpha} + \nu u_{\alpha,jj}. \tag{4}$$

Here $\mathbf{U}$ is the mean velocity vector, p the fluctuating kinematic pressure and ν the kinematic viscosity. A subscript comma denotes differentiation and repeated non-Greek indices are summed. Multiplying (4) by $2nu_\alpha^{2n-1}$ and averaging gives

$$\partial\langle u_\alpha^{2n}\rangle/\partial t = \underbrace{-2nU_{\alpha,j}\langle u_j u_\alpha^{2n-1}\rangle}_{\text{shear production}} \underbrace{- U_j\langle (u_\alpha^{2n})_{,j}\rangle}_{\text{advection}} \underbrace{- \langle (u_\alpha^{2n}u_j)_{,j}\rangle}_{\text{turbulent transport}}$$
$$\underbrace{+2n\langle u_\alpha^{2n-1}\rangle\langle (u_\alpha u_j)_{,j}\rangle}_{\text{turbulent production}} \underbrace{- 2n\langle u_\alpha^{2n-1}p_{,\alpha}\rangle}_{\text{pressure interaction}} \underbrace{+ 2n\nu\langle u_\alpha^{2n-1}u_{\alpha,jj}\rangle}_{\text{viscous effects}}. \tag{5}$$

Equation (5) shows that $\langle u_\alpha^{2n}\rangle$ is maintained by a variety of terms. Their relative importance can be determined from scaling arguments of the type used, for example, in Tennekes & Lumley (1972, p. 63) and by considering the form of the $\langle u_\alpha^{2n}\rangle$ equation in special cases. Taking the scaling arguments first, we note that the time rate of change term is at most of order

$$\frac{\partial}{\partial t}\langle u_\alpha^{2n}\rangle \sim \frac{q^{2n}}{l/q} \sim \frac{q^{2n+1}}{l}, \tag{6}$$

where q and l are velocity and length scales of the energy-containing eddies. The first four terms on the right side can also be shown to be at most of this order.

To evaluate the viscous term we start by noting that molecular diffusion of $\langle u_\alpha^{2n}\rangle$ is negligible in large Reynolds number turbulence:

$$\nu\langle (u_\alpha^{2n})_{,jj}\rangle \sim \frac{\nu q^{2n}}{l^2} \sim \frac{q^{2n+1}}{l}\frac{\nu}{lq} \sim \frac{q^{2n+1}}{l}R_l^{-1}, \tag{7}$$

where $R_l = ql/\nu$ is a turbulence Reynolds number. We exploit this result by writing

$$(\nu l/q^{n+1})\langle (u_\alpha^{2n})_{,jj}\rangle \simeq 0 \tag{8}$$

and manipulating this to get

$$\langle u_\alpha^{2n-1} u_{\alpha,jj}\rangle = -(2n-1)n^{-2}\langle u^n_{\alpha,j} u^n_{\alpha,j}\rangle. \tag{9}$$

Using (9), the viscous term in the $\langle u_\alpha^{2n}\rangle$ budget (5) becomes

$$2n\nu\langle u_\alpha^{2n-1} u_{\alpha,jj}\rangle = -2\nu(2n-1)n^{-1}\langle u^n_{\alpha,j} u^n_{\alpha,j}\rangle, \tag{10}$$

which shows that it is always negative and hence represents viscous destruction.

To determine the magnitude of the viscous destruction, we note that

$$\langle u^n_{,j} u^n_{,j}\rangle = n^2\langle u^{n-1}u^{n-1}u_{,j}u_{,j}\rangle. \tag{11}$$

We have dropped the subscript α since the arguments for this term will hold for any component. The higher-order spectral results show that the dominant Fourier modes of $u^{n-1}u^{n-1}$ lie in the energy-containing (small wavenumber) range, and earlier work (e.g. Wyngaard & Pao 1972) shows that those of $u_{,j}u_{,j}$ lie in the large wavenumber range. It is believed (see, for example, Tennekes & Lumley 1972) that these two ranges approach statistical independence as the turbulence Reynolds number (and hence their separation) increases. We write, therefore,

$$\langle u^{n-1}u^{n-1}u_{,j}u_{,j}\rangle \sim \langle u^{n-1}u^{n-1}\rangle\langle u_{,j}u_{,j}\rangle \sim q^{2n}/\lambda^2, \tag{12}$$

where $\lambda = (\nu l/q)^{\frac{1}{2}}$ is the Taylor microscale. Our estimate for viscous destruction then is, from (10)–(12),

$$\nu\langle u^n_{\alpha,j} u^n_{\alpha,j}\rangle \sim \nu q^{2n}/\lambda^2 \sim q^{2n+1}/l, \tag{13}$$

which indicates that viscous destruction is of the order of the largest terms in the budget.

The dominant role of viscosity can also be inferred directly in special cases. For example, in a boundary layer over a flat surface and for $\alpha = 2$ (the lateral direction), the shear production, advection and turbulent production terms in (5) all vanish. Turbulent transport only moves $\langle u_\alpha^{2n}\rangle$ around in space, since it integrates to zero over the whole flow. In this flow, then, the pressure and viscous terms are the dominant source and sink, respectively, for $\langle v^{2n}\rangle$.

The dominant role of viscous destruction has direct implications for higher-order spectra. If we use a Fourier–Stieltjes representation for the nth moment,

$$u^n - \langle u^n\rangle = \int e^{i\mathbf{k}.\mathbf{x}} dZ_n(\mathbf{k}), \quad \langle dZ_n(\mathbf{k})\, dZ_n^*(\mathbf{k})\rangle = \phi_n(\mathbf{k})\, d\mathbf{k}, \tag{14}$$

then it follows that

$$\left.\begin{aligned} \langle (u^n - \langle u^n\rangle)^2\rangle &= \int \phi_n(\mathbf{k})\, d\mathbf{k}, \\ \langle (u^n - \langle u^n\rangle)_{,j}\rangle\langle (u^n - \langle u^n\rangle)_{,j}\rangle &= \int k^2\phi_n(\mathbf{k})\, d\mathbf{k}. \end{aligned}\right\} \tag{15}$$

We can also write

$$\langle (u^n - \langle u^n\rangle)_{,j}(u^n - \langle u^n\rangle)_{,j}\rangle = \langle u^n_{,j}u^n_{,j}\rangle - \langle u^n_{,j}\rangle\langle u^n_{,j}\rangle. \tag{16}$$

The second term on the right side of (16) is smaller than the first by a factor

$\lambda^2/l^2 \sim R_l^{-1}$ and can be neglected. It follows that the viscous destruction rate of $\langle u^{2n}\rangle$ (call it ϵ_{2n}) is

$$\epsilon_{2n} = \frac{2(2n-1)}{n}\nu\int k^2\phi_n(\mathbf{k})\,d\mathbf{k}. \tag{17}$$

We said earlier that the dominant contributions to ϵ_{2n} come from the largest wavenumbers. If there is an inertial range where $\phi_n \sim k^{-m}$, it follows that $m < 2$.

The budget for the odd moment $\langle u^{2n+1}\rangle$ is derived in the same way. It reads

$$\partial\langle u_\alpha^{2n+1}\rangle/\partial t = \underset{\text{shear production}}{-(2n+1)\,U_{\alpha,j}\langle u_j u_\alpha^{2n}\rangle} \underset{\text{advection}}{-U_j\langle(u_\alpha^{2n+1})_{,j}\rangle} \underset{\text{turbulent transport}}{-\langle(u_\alpha^{2n+1}u_j)_{,j}\rangle}$$
$$+\underset{\text{turbulent production}}{(2n+1)\langle u_\alpha^{2n}\rangle\langle(u_\alpha u_j)_{,j}\rangle} \underset{\text{pressure interaction}}{-(2n+1)\langle u_\alpha^{2n}p_{\,\alpha}\rangle}$$
$$\underset{\text{viscous effects}}{-(2n+1)\,\nu\langle(u_\alpha^{2n})_{,j}u_{\alpha,j}\rangle}. \tag{18}$$

The dominant terms here are of order q^{2n+2}/l. If the correlation between u_α^{2n} and u_α extends throughout the k range, then the viscous term is of the same order:

$$\nu\langle(u_\alpha^{2n})_{,j}u_{\alpha,j}\rangle \simeq \nu\frac{q^{2n}}{\lambda}\frac{q}{\lambda} \approx \frac{q^{2n+2}}{l}. \tag{19}$$

Note that the viscous term can be expressed in terms of the higher-order cospectrum:

$$(2n+1)\,\nu\langle(u_\alpha^{2n})_{,j}u_{\alpha,j}\rangle = (2n+1)\,\nu\int k^2 C_0(u_\alpha^{2n},u_\alpha)\,d\mathbf{k} = \epsilon_{2n+1}. \tag{20}$$

Viscous destruction will be confined to the high-k range, and hence will be significant if the cospectrum falls slower than k^{-2} in the inertial range.

The picture we have roughly sketched suggests that the familiar ideas about the maintenance of velocity variance in large R_l turbulence, and the roles the various scales of motion play, can be generalized to higher moments. Production occurs mainly in the energy-containing (low k) range, with viscous destruction confined to large k. If R_l is so large that these ranges are sufficiently separated, we expect an intermediate, inertial range where only transfer from smaller to larger k occurs.

Direct application of the Kolmogorov arguments to these higher-order spectra gives

$$\left.\begin{aligned} C_0(u^{2n},u) &= f(\epsilon,k) = \epsilon^{\frac{1}{3}(2n+1)}k^{-(\frac{4}{3}+\frac{2}{3}n)},\\ \phi_n &= g(\epsilon,k) = \epsilon^{\frac{2}{3}n}k^{-(\frac{2}{3}n+1)}.\end{aligned}\right\} \tag{21}$$

These are clearly incorrect: the slopes are too steep compared with experimental values and the cospectrum does not change sign under co-ordinate reflexion as it must.

A natural extension of the Kolmogorov ideas, and one which recognizes the importance of viscous destruction for higher moments, is

$$C_0(u^{2n},u) = f(\epsilon,\epsilon_{2n+1},k), \quad \phi_n = g(\epsilon,\epsilon_{2n},k). \tag{22}$$

If ϕ_n and C_0 depend in the same way on their arguments, the simplest forms with the required property under co-ordinate reflexion are

$$C_0(u^{2n},u) \simeq \epsilon_{2n+1}\epsilon^{-\frac{1}{3}}k^{-\frac{5}{3}}, \quad \phi_n \simeq \epsilon_{2n}\epsilon^{-\frac{1}{3}}k^{-\frac{5}{3}}. \tag{23}$$

This predicts that the coherence between u^{2n} and u in the inertial range is independent of the wavenumber. It is also interesting to note the similarity between the higher-order predictions of (23) and that of Corrsin (1951) for the inertial-range spectral level of a passive scalar θ:

$$\phi_\theta \sim N\epsilon^{-\frac{1}{3}}k^{-\frac{5}{3}}, \tag{24}$$

where N is the rate of destruction of scalar variance.

2.2. *Higher-order inertial-subrange spectra for a Gaussian variable*

The dimensional arguments given in §2.1 can predict only the functional dependence of the higher-order spectra on the wavenumber, and not their magnitudes. In this section, an alternative analysis, based on the assumption of Gaussianity, yields predictions for all spectral levels, and gives the same dependence upon wavenumber, which is invariant for all higher-order spectra.

For convenience of comparison with the raw experimental data, the following theoretical development is carried out in terms of spectra that are a function of the frequency f (measured in Hz), rather than in terms of a spatial wavenumber k. Since the measured velocity fluctuations are assumed to be stationary random functions of the time t, comparisons with the predictions of the Gaussian theory can be made without recourse to an assumed relation between f and k. However, when the analytical results are compared with predictions like (2) and (23), it is to be understood that Taylor's hypothesis (see Hinze 1959, p. 40) in the form $k = f/U$ has been invoked, where U is the mean flow velocity.

If a stationary random function of time $u(t)$ is normally distributed, then the higher-order spectra ϕ_n of $u^n(t)$ defined by (1) can all be computed in principle from a knowledge of only the first-order spectrum ϕ_1, or its corresponding correlation function $R(\tau)$. This result follows from the fact that, for a Gaussian process, the joint statistics of the bivariate distribution for $u(t)$ and $u(t+\tau)$ are completely determined by the correlation function $R(\tau) = \langle u(t)\,u(t+\tau)\rangle$. Given the two-sided power spectrum $\phi_1(f)$ of $u(t)$, we wish to find the power spectrum $\phi_n(f)$ of $u^n(t)$. The power spectrum $\phi_n(f)$ will be equal to the inverse Fourier transform of the correlation function $\langle u^n(t)\,u^n(t+\tau)\rangle$:

$$\phi_n(f) = \int_{-\infty}^{\infty} \langle u^n(t)\,u^n(t+\tau)\rangle\, e^{-i2\pi f\tau}\,d\tau. \tag{25}$$

For odd powers of $u(t)$, we have (see, for example, Rice 1973)

$$\langle u^{2n+1}(t)\,u^{2n+1}(t+\tau)\rangle = \sum_{k=0}^{n} \frac{[(2n+1)!]^2\, R^{2k+1}(\tfrac{1}{2}R(0))^{2n-2k}}{(2k+1)!\,[(n-k)!]^2},$$

where

$$R(0) = \int_{-\infty}^{\infty} \phi_1(f)\,df = \langle u^2(t)\rangle$$

is the variance. For even n, say $n = 2m$, a similar calculation yields

$$\langle u^{2m}(t)\,u^{2m}(t+\tau)\rangle = \sum_{k=0}^{m} \frac{[(2m)!]^2\, R^{2m-2k}(\tfrac{1}{2}R(0))^{2k}}{(k!)^2\,(2m-2k)!}.$$

The higher-order spectra of a Gaussian variable are thus given by

$$\phi_{2n+1}(f) = \int_{-\infty}^{\infty} d\tau\, e^{-i2\pi f\tau} \sum_{k=0}^{n} \frac{[(2n+1)!]^2 R(\tau)^{2k+1}(\frac{1}{2}R(0))^{2n-2k}}{(2k+1)!\,[(n-k)!]^2} \quad \text{(odd powers of } u(t)), \qquad (26)$$

$$\phi_{2m}(f) = \int_{-\infty}^{\infty} d\tau\, e^{-i2\pi f\tau} \sum_{k=0}^{m} \frac{[(2m)!]^2 R(\tau)^{2m-2k}(\frac{1}{2}R(0))^{2k}}{(k!)^2\,(2m-2k)!} \quad \text{(even powers of } u(t)). \qquad (27)$$

The manipulation of these relations that follows makes use of the convolution relation for the Fourier transform of powers of the correlation function:

$$\int_{-\infty}^{\infty} R^m(\tau)\, e^{-i2\pi f\tau} d\tau = \int_{-\infty}^{\infty} df_1 \cdots \int_{-\infty}^{\infty} df_{m-1} \phi_1(f_1) \cdots \phi_1(f_{m-1})\, \phi_1(f-f_1 \cdots f_{m-1})$$
$$= (m-1)\text{-fold convolution of } \phi_1(f). \qquad (28)$$

In the general case, evaluation of the higher-order spectra of a Gaussian variable requires either analytical or numerical evaluation of the integrals in (26) and (27), or evaluation of the convolution integrals in (28). These operations require that the entire spectrum or correlation function be specified. However, for the present atmospheric data, we are mainly interested in the behaviour of the spectra in the inertial subrange. As observed by Kaimal *et al.* (1972), first-order spectra obtained from different experiments and under different conditions show a wide systematic variation for low frequencies, depending on the degree of stability and other external parameters, but their forms and magnitudes in the inertial subrange follow a universal scaling. An asymptotic analysis for large frequencies, applying only to the inertial subrange, appears desirable.

To carry out the analysis, one needs a spectral form which reduces to the Kolmogorov spectrum for large frequencies or wavenumbers. A suitable form, due to von Kármán and discussed by Hinze (1959, p. 199), is

$$\phi_1(f) = b\lambda^{\frac{5}{3}}/[1+(\lambda f)^2]^{\frac{5}{6}}. \qquad (29)$$

It seems likely that other model spectra which have a $k^{-\frac{5}{3}}$ behaviour in the inertial subrange would also be suitable for the present purpose. The von Kármán spectrum has the advantage of possessing a simple and convenient correlation function (see appendix), which makes it fairly easy to carry out an asymptotic analysis for large f. From (29), the mean square of the velocity fluctuations is

$$\langle u^2 \rangle \equiv R(0) = b\lambda^{\frac{2}{3}}[\Gamma(\tfrac{1}{2})\,\Gamma(\tfrac{1}{3})/\Gamma(\tfrac{5}{6})] = 4{\cdot}20 b\lambda^{\frac{2}{3}}. \qquad (30)$$

The higher-order spectra for odd powers of $u(t)$ are then given by

$$\phi_{2m+1}(f) = [(2m+1)!]^2 \sum_{k=0}^{m} \left(\frac{4{\cdot}20 b\lambda^{\frac{2}{3}}}{2}\right)^{2m-2k} \frac{(2k\text{th convolution of } \phi_1)}{(2k+1)!\,[(m-k)!]^2}.$$

For large values of f, keeping only the leading term in the $2k$th convolution of ϕ_1 gives (see appendix)

$$2k\text{th convolution of } \phi_1(f) \sim b(b\lambda^{\frac{2}{3}})^{2k}(4{\cdot}20)^{2k}(2k+1)f^{-\frac{5}{3}}$$
$$+ \text{(higher-order terms in } f).$$

So for large f, the dependence on f will be the same ($\phi_n \sim f^{-\frac{5}{3}}$) for higher-order spectra of all orders. We then have for large f

$$\phi_{2m+1}(f) \sim [(2m+1)!]^2 b f^{-\frac{5}{3}} \left(\frac{4{\cdot}20 b\lambda^{\frac{2}{3}}}{2}\right)^{2m} \sum_{k=0}^{m} \frac{1}{k!(\frac{1}{2})_k [(m-k)!]^2}.$$

The summation term can be written as

$$\sum_{k=0}^{m} \frac{(-1)^{2k}(-m)_k(-m)_k}{k!(\frac{1}{2})_k (m!)^2} = \frac{F(-m,\ -m;\ \frac{1}{2};\ 1)}{(m!)^2}$$
$$= \frac{\Gamma(\frac{1}{2})\,\Gamma(\frac{1}{2}+2m)}{(m!)^2\,\Gamma(\frac{1}{2}+m)\,\Gamma(\frac{1}{2}+m)} = \frac{(\frac{1}{2})_{2m}\,2^{2m}}{[(2m)!]^2}.$$

Finally, for the power spectra of odd powers of $u(t)$ we have

$$\phi_{2m+1}(f) \sim b(4{\cdot}20 b\lambda^{\frac{2}{3}})^{2m}(2m+1)^2[1 \times 3 \times 5 \times \ldots \times (4m-1)] f^{-\frac{5}{3}} \quad (m = 1, 2, \ldots). \tag{31}$$

A similar analysis for even powers of $u(t)$ produces the result

$$\phi_{2m}(f) \sim (\text{d.c. spike}) + b(4{\cdot}2 b\lambda^{\frac{2}{3}})^{2m-1} \times (2m)^2[1 \times 3 \times 5 \times \ldots \times (2m-1)(2m+1) \times \ldots \times (4m-3)] f^{-\frac{5}{3}}. \tag{32}$$

Equations (31) and (32) may be combined to obtain a single expression valid for arbitrary powers (both even and odd) of u:

$$\phi_n(f) \sim (\text{d.c. spike if } n \text{ is even}) + b(4{\cdot}2 b\lambda^{\frac{2}{3}})^{n-1} n^2[1 \times 3 \times 5 \times \ldots \times (2n-3)] f^{-\frac{5}{3}}, \tag{33}$$

where the final product in brackets is replaced by 1 when $n = 1$.

From (29) and (33), the non-dimensionalized ratio of the higher-order spectra to the first-order spectrum is simply

$$\phi_n(f)/[R(0)^{n-1}\phi_1(f)] = n^2[1 \times 3 \times 5 \times \ldots \times (2n-3)]. \tag{34}$$

Note that this ratio is independent of the parameters b and λ and of the dimensions used for the velocity u and other multiplicative constants in the spectra or frequency variable.

3. Comparison of atmospheric experimental data with theory

The raw computed spectra shown in figures 1 and 2 were compared with the dimensional theory of §2.1 and with the asymptotic theory of §2.2. These are spectra of the longitudinal component $u(t)$ of the fluctuating velocity obtained in the atmospheric boundary layer over the open ocean at a height of 3 m above the mean water surface level. The data were obtained during steady trade wind conditions from FLIP, the stable floating instrument platform of the Scripps Institution of Oceanography, during the Barbados Oceanographic and Meteorological Experiment (BOMEX), in May 1969. The mean velocity was 7·2 m/s. The fluctuating velocity was measured with a single vertically oriented hot wire 5 μm in diameter and 1 mm long. This hot wire was operated in the constant-resistance

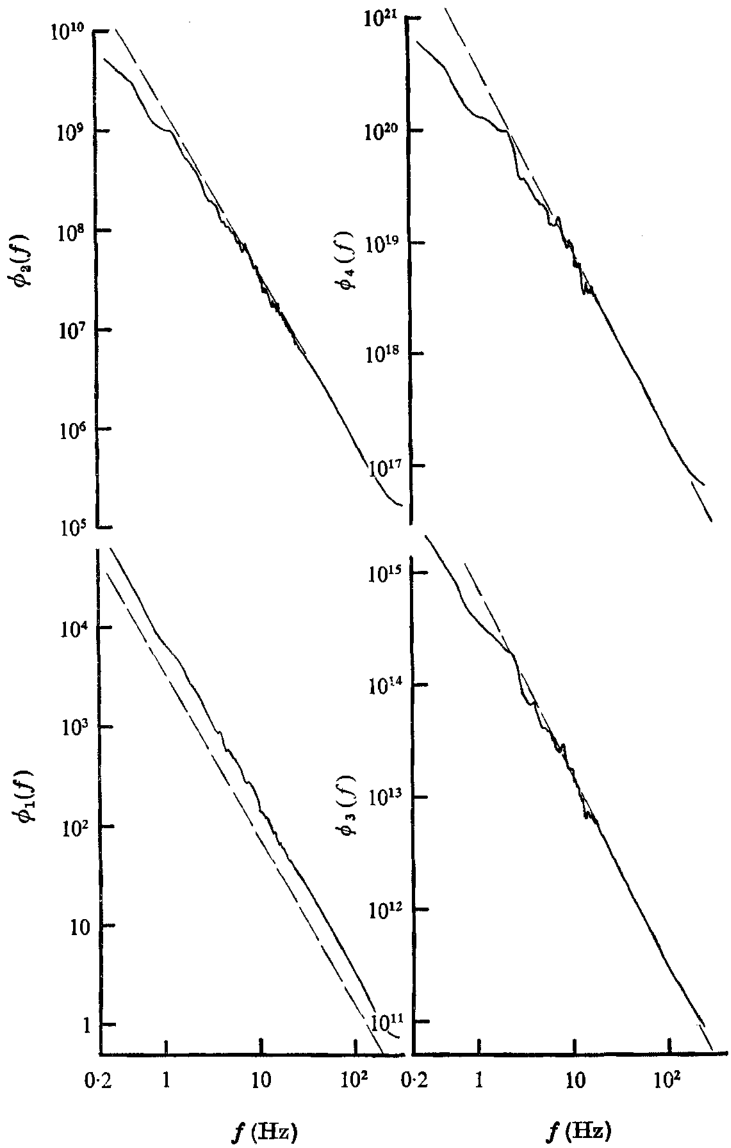

FIGURE 1. First-, second-, third- and fourth-order spectra of $u(t)$ measured in the atmospheric boundary layer over the open ocean. Dashed lines, which have a slope of $-\frac{5}{3}$, are higher-order inertial-subrange spectra predicted by asymptotic Gaussian theory. Dashed $-\frac{5}{3}$ line in ϕ_1 plot is not a fit to data. Note large range of the magnitudes of the higher-order spectra.

mode using a DISA 55D05 anemometer, and the anemometer output was linearized with a DISA 55D10 linearizer. The linearized hot-wire signal was FM tape recorded and later played back and sampled in the laboratory with a 12-bit analog-to-digital converter at a rate of 521·5 samples/s. Further details of the experimental conditions and apparatus, calibrations and data sampling have been given by Van Atta & Chen (1970) and Van Atta & Park (1972) in studies of

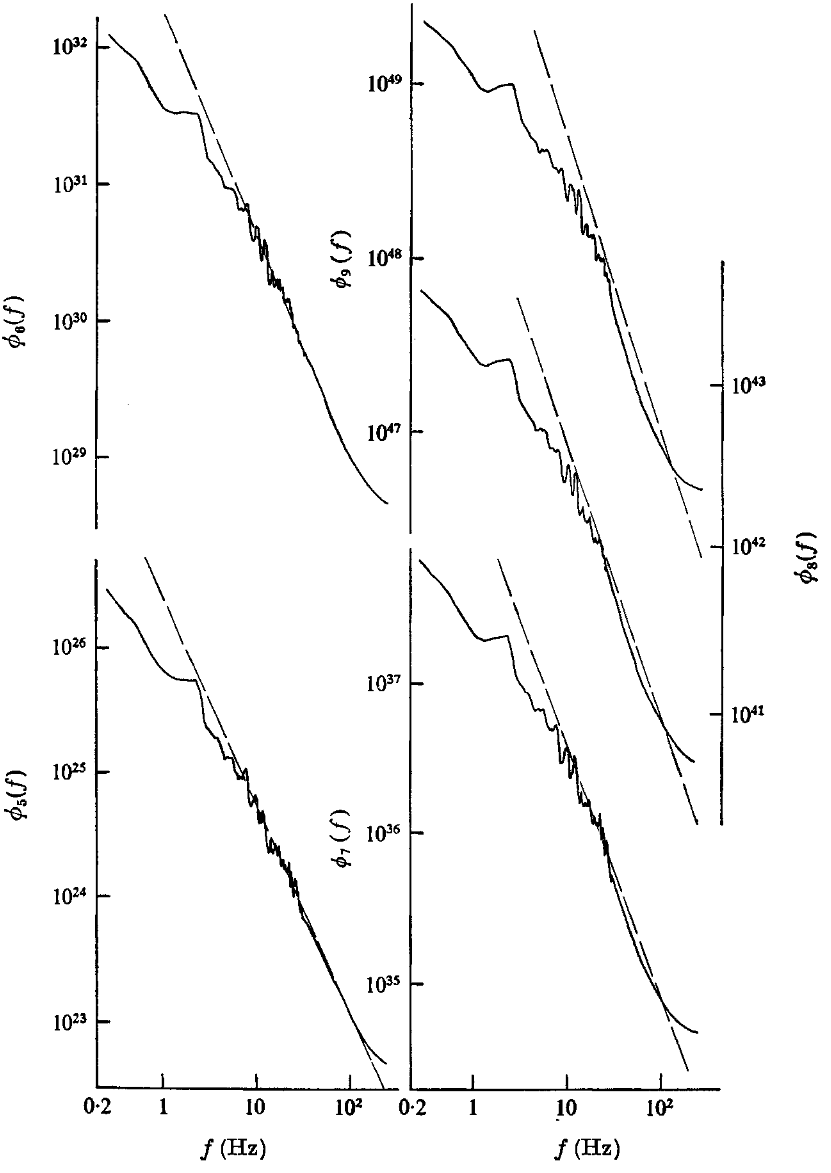

FIGURE 2. Fifth-, sixth-, seventh-, eighth- and ninth-order inertial-subrange spectra of $u(t)$ measured in the atmospheric boundary layer over the open ocean. Dashed lines have same meaning as in figure 1.

structure functions in the inertial subrange. The present spectra were obtained using fast Fourier transforms of 100 digital records, each of which contained 2048 samples. Individual record averages of u^n were used for the mean values $\langle u^n \rangle$. For atmospheric data, individual record averages of such short length will fluctuate considerably around the long-term average. Use of the long-term averages to compute the fluctuations and spectral levels in each record will produce errors in the measured higher-order spectra that depend on the values of lower-order spectra. For example, if in a given record the local record mean differs from the long-term mean by u_0, i.e. $u(t) = u_0 + \tilde{u}$, where $\langle \tilde{u} \rangle = 0$, then

$$\phi_{2(u^2,u^2)}(f) = \phi_{2(\tilde{u}^2,\tilde{u}^2)}(f) + 4u_0^2\phi_{1(\tilde{u},\tilde{u})}(f) + 2u_0(S_{\tilde{u},\tilde{u}^2}(f) + S_{\tilde{u}^2,\tilde{u}}(f)),$$

where $S_{\tilde{u},\tilde{u}^2}$ is the cross-spectrum of $\tilde{u}$ and $\tilde{u}^2$. The measurement of ϕ_2 is thus contaminated by terms that are proportional to ϕ_1 and S. For measurements of ϕ_1, the value of u_0 affects only the zero-frequency spectral value $\phi(0)$. For laboratory data, the record length can normally be chosen to be considerably longer (say by a factor of 10 or 20) than the integral time scale of the fluctuations, and the spectral contamination problem is negligible because of the small size of the residual u_0. Attention was first drawn to this kind of problem by Chen (1969) in connexion with correlation measurements, for which record means are not appropriate. A discussion of similar questions concerning cross-spectral measurements has been given by Helland (1974).

The data shown in figures 1 and 2 are spectral averages over 100 records. In these data, a clear $-\frac{5}{3}$-power-law range in the spectra is apparent for all spectra of up to sixth order, but for higher orders it is not as clearly defined, partly owing to an increasing oscillation in the spectra near 30 Hz. The effect of aliasing in the high frequency tails of the spectra also becomes more apparent as the order is increased. The slopes of the dashed lines $(-\frac{5}{3})$ are those predicted both by the asymptotic Gaussian theory and the present extension of Kolmogorov's dimensional theory [equation (33)]. The dashed lines also denote the absolute spectral values predicted by the Gaussian theory (except in figure 1*a*). The present theories both represent the data fairly well. The present generalized Kolmogorov theory clearly provides a good representation of the data, in contrast to the earlier proposal for inertial-subrange behaviour by Dutton & Deaven [equation (2)]. The frequency below which the spectra depart from an approximately $-\frac{5}{3}$ slope increases monotonically with increasing order. For high frequencies, the measured spectra are thus in qualitative agreement with the Gaussian asymptotic theory and with the trends observed by Dutton & Deaven.

The asymptotic theory was compared quantitatively with the present experiments by using the measured lower-order spectra to determine the constants b and λ and then comparing the measured higher-order spectra with their predicted magnitudes obtained using the same values of b and λ. The data for the frequency range 10–100 Hz were used in determining b and λ. A fit to the data for ϕ_1 in figure 1 gives $b = 7194$, corresponding to a value of $\phi_1 = 155$ at $f = 10$ Hz. Using this value of b, the values of λ determined from ϕ_2 and ϕ_3 are $\lambda = 2{\cdot}6$ and $3{\cdot}0$, respectively. The average of these two values, $\lambda = 2{\cdot}8$, was then used with $b = 7194$ to predict the values of the higher-order spectra using (33).

The fits for the lower-order spectra and the predicted spectra for higher orders are indicated by the dashed lines in figures 1 and 2 for $2 \leqslant n \leqslant 9$. In most cases the predicted spectral levels indicated by the dashed lines pass directly through the measured spectral values, and are in fact close approximations to the measured spectra for each value of n. In view of the large changes in the absolute spectral level with increasing n, the agreement between the asymptotic formula (33) and the measured spectra in the $-\frac{5}{3}$ range appears to be quite good. For

$n = 8$ and 9, the predicted levels are a bit high. For the largest values of n the spectra are also becoming progressively more ragged and the $-\frac{5}{3}$ range is not clearly defined. From the present data, one may conclude that, for the spectra of up to and including seventh order, the measured spectra in the inertial range are in good agreement with theoretical predictions for higher-order spectra of a Gaussian variable.

For the present data, the extent of the $-\frac{5}{3}$-slope region in the spectra is less for all higher-order spectra than for the first-order spectrum. For comparison with the low-frequency ends of spectra predicted using the von Kármán form for ϕ_1, the complete higher-order spectra for $n \leqslant 4$ were determined numerically. Using the normalized correlation function [see equation (A 1) of the appendix]

$$R(\tau)/R(0) = 2^{\frac{2}{3}}(2\pi\tau/\lambda)^{\frac{1}{3}}K_{\frac{1}{3}}(2\pi\tau/\lambda)/\Gamma(\tfrac{1}{3})$$

the expressions in (26) and (27) were numerically evaluated using a fast-Fourier-transform routine. These numerical results also served as a further check on the asymptotic theory for large f. The second-order spectrum was also evaluated using a direct numerical convolution, as a further check on the calculations performed via sums of Fourier transforms of powers of the correlation function. It did not appear practical to attempt to obtain ϕ_n for $n > 2$ by numerically evaluating the multiple convolutions of (28). The results of these calculations, which are applicable for arbitrary values of b and λ, are shown in figure 3. The numerical results are in good agreement with the asymptotic theory, and show that for a von Kármán spectrum the asymptotic theory is a good approximation down to dimensionless frequencies $F = f\lambda$ of about 10, the lower limit being a weakly increasing function of the order of the spectrum. This latter behaviour is consistent with that observed in the data.

The measured probability density of the velocity fluctuations is shown in figure 4. Although the distribution is decidedly non-Gaussian, the deviations from Gaussianity are small enough so that the first few moments are of the same order of magnitude as those for a Gaussian distribution. For a Gaussian distribution, and therefore also for the numerically determined spectra in figure 3, the values of the moments are given by $\langle u^{2n}\rangle/\langle u^2\rangle^n = 1\times 3\times 5\times \ldots \times(2n-1)$. In view of (1), the ratios of the areas under all the higher-order spectral curves are therefore fixed. However, as the order increases, the moments will rapidly deviate from those expected for a Gaussian density. As is well known, experimental values of such moments are a strong function of the type of flow, stability and the position of measurement in the flow (e.g. the distance from the boundary in a boundary layer). The present good agreement between the Gaussian calculations of ϕ_n and experimental values in the inertial subrange indicates that the major contribution to non-Gaussian behaviour of the higher-order moments comes from the non-universal low-frequency end of the first-order and higher-order spectra. Higher-order moments and the corresponding low-frequency portion of the higher-order spectra have not been determined for the present atmospheric data. This would require lower sampling rates and considerably longer samples of data than were used for the inertial-subrange spectral calculations.

The Dutton & Deaven data are most easily compared with the asymptotic

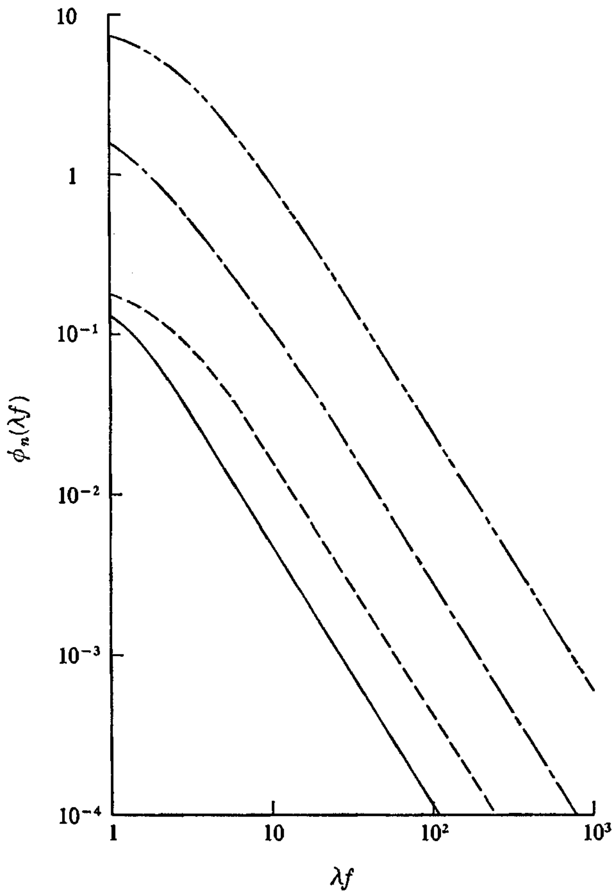

FIGURE 3. Numerically computed first-, second-, third- and fourth-order spectra obtained using Gaussian theory and normalized correlation function of von Kármán spectrum. Note departure from inertial-subrange behaviour for low frequencies and decrease in extent of inertial-subrange $(-\frac{5}{3})$ behaviour as order of spectrum increases. ——, ϕ_1; – – –, ϕ_2; — · —, ϕ_3; — ·· —, ϕ_4.

theory using (34). In processing their data, Dutton & Deaven worked with the velocity normalized with its variance, i.e. $u/R_u(0)^{\frac{1}{2}}$, $v/R_v(0)^{\frac{1}{2}}$, etc., and the spectral data they presented are also given in terms of the velocity components normalized with their variances. For this reason, the ratio of any of their spectral results to their first-order spectrum corresponds exactly to the definition of the dimensionless spectrum given in (34). We therefore can simply multiply their first-order spectrum by 4, 27 and 60 in order to compare their experimental results with the asymptotic theory for ϕ_2, ϕ_3 and ϕ_4, respectively. Results of this comparison are illustrated in figure 5, which is a replot of the Dutton & Deaven LO-LOCAT 750 ft data. These data exhibited the most regular behaviour in the inertial subrange, and appear to be the most suitable of their data for the present comparison. The asymptotic theory predicts the magnitudes of the higher-order spectra quite well, and the agreement is as good as one could hope for, considering the relatively small extent of the inertial subrange covered by the data. These measured spectra

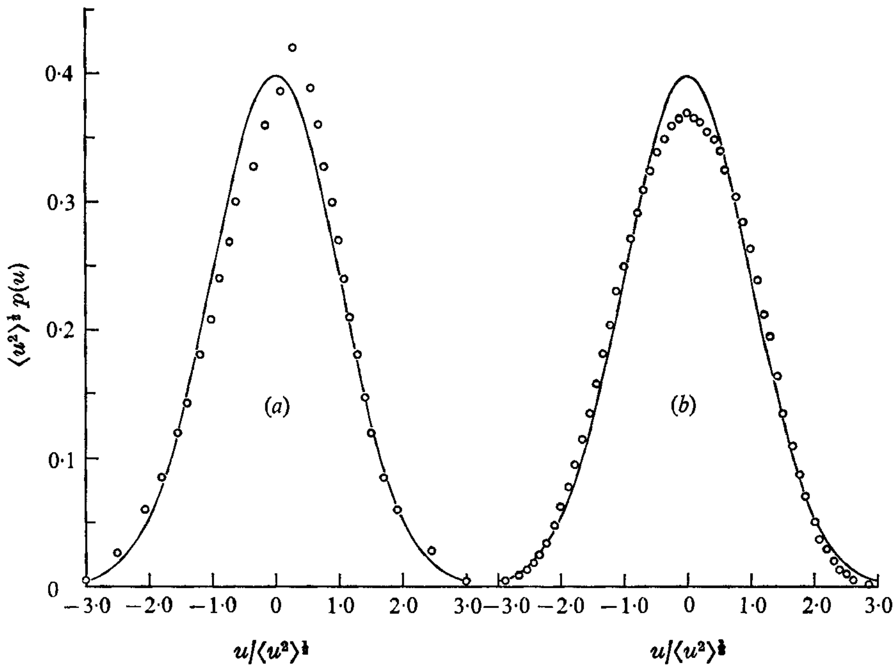

FIGURE 4. Probability densities of $u(t)$ for present atmospheric boundary-layer data and mixing-layer centre-line data of Champagne *et al.* (*a*) Atmospheric boundary layer over the open ocean. (*b*) Two-dimensional mixing layer. ——, Gaussian distribution.

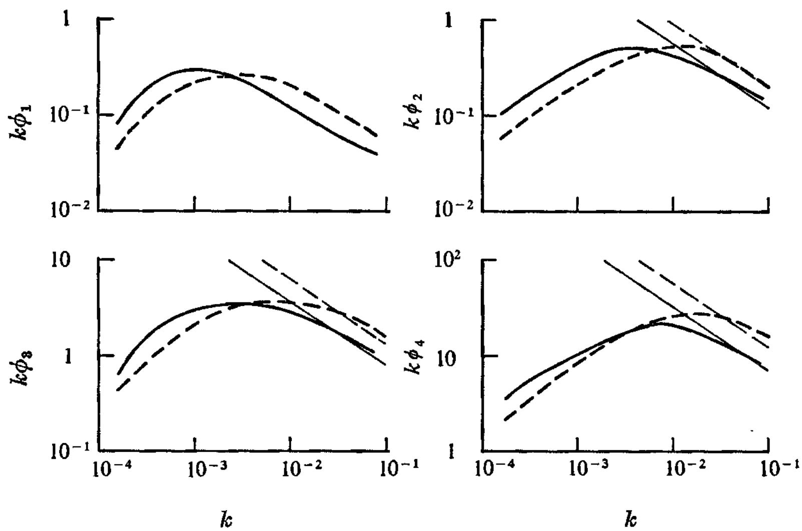

FIGURE 5. First-, second-, third- and fourth-order spectra $k\phi_n(k)$ obtained by Dutton & Deaven for the LO-LOCAT 750 ft (altitude) data. The straight lines, which have a slope of $-\frac{2}{3}$, are higher-order inertial-subrange spectra predicted by asymptotic Gaussian theory using the von Kármán spectral form. Note that in these co-ordinates the $-\frac{2}{3}$ slope corresponds to the $-\frac{5}{3}$ power law of Kolmogorov theory. ——, u, longitudinal component of velocity; – – –, v, lateral component of velocity.

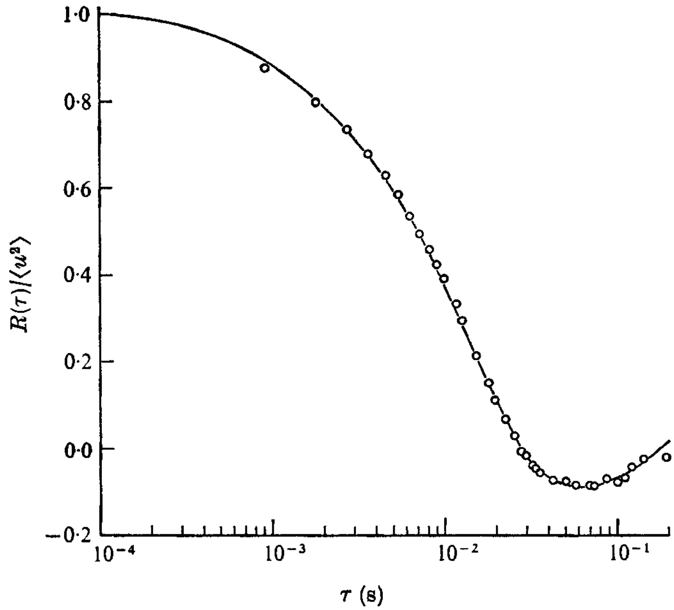

FIGURE 6. Curve fit to plane-mixing-layer correlation-function data used for numerical computations of higher-order spectra shown in figure 7. ——, curve fit; ○, data of Champagne *et al.*

also exhibit the trend that the inertial-subrange spectral behaviour begins at a higher frequency as the order of the spectrum increases. This is consistent with the trend in the BOMEX data and with that predicted by the calculations using the von Kármán spectral model.

4. Comparison of Gaussian theory with some laboratory data

Laboratory measurements on the centre-line of a plane mixing layer of spectra of $u^n(t)$ up to fourth order have been made recently by Champagne *et al.* (1976). Their measurements were motivated by a need to determine whether the frequency response of their analog and digital measuring instruments and computational techniques was adequate for determining the higher-order moments of $u(t)$. Since raising a signal to a power (e.g. squaring) produces sum and difference frequencies, this operation produces higher-order spectral energy at frequencies considerably exceeding the usual Nyquist frequency. As discussed by Van Atta (1974), if the first-order spectrum does not fall sufficiently rapidly, higher-order spectral mass can be lost if the data are processed according to the usual Nyquist criterion. Champagne *et al.* found that in their case this was not a serious problem, and that their measured spectra gave an accurate measure of the contributions of various frequency components to the higher-order moments. Their first-order spectrum exhibited a small interval of roughly $f^{-\frac{5}{3}}$ behaviour. They noted that in this frequency interval their higher-order spectra did not follow the trend predicted by (2), but rather the spectra became somewhat less steep (on a log–log plot) as the order increased.

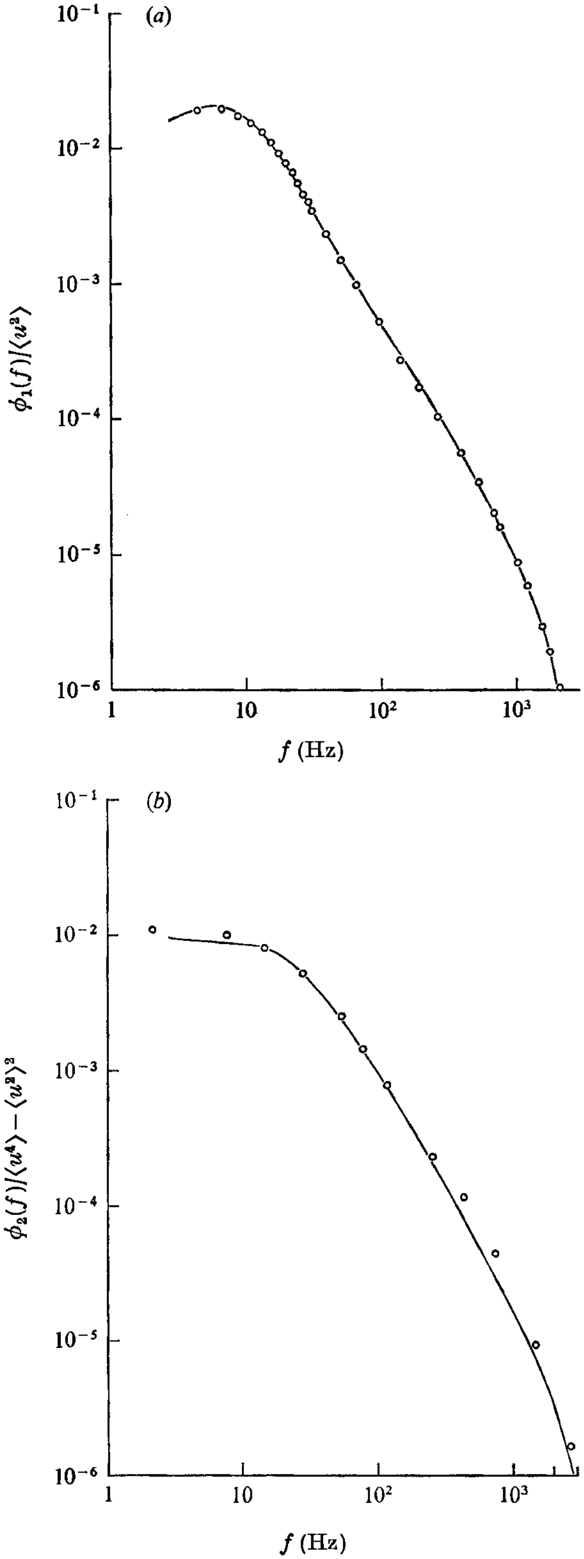

FIGURES 7 (*a*, *b*). For legend see next page.

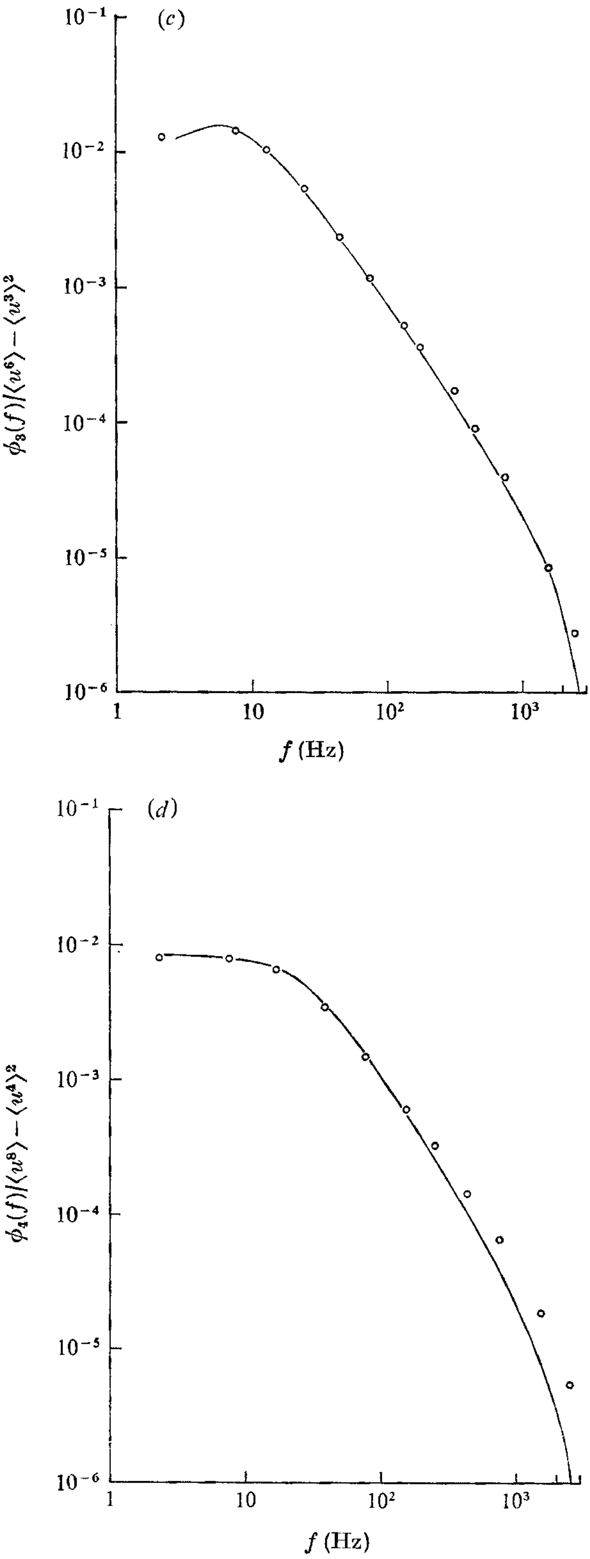

FIGURE 7. (*a*) First-, (*b*) second-, (*c*) third- and (*d*) fourth-order normalized spectra for plane-mixing-layer centre-line data. ——, numerical Fourier transform using correlation-function curve fit of figure 6; ○, data of Champagne *et al.*

Theoretical higher-order spectra for the mixing-layer data were computed from (26) and (27), using a three-section polynomial curve fit to the measured correlation function as input to the same program as was used to produce the data in figure 3. The curve fit shown in figure 6 was used to generate 4096 points of the correlation function. Some numerical experimentation with the curve fit for small time lags τ was necessary in order to fit accurately the high-frequency end of the first-order spectrum, as only a few points were available for the measured correlation function for small τ. These correlation data were then raised to the appropriate powers and fast Fourier transformed to generate the terms in (26) and (27). Since spectra up to only fourth order were computed, this procedure required a maximum of two Fourier transforms for each higher-order spectrum computed. The resulting spectra are shown in figures 7 (*a*)–(*d*). The computed results for ϕ_1 are in close agreement with the measured spectrum, indicating that the fit to the correlation function is adequate, and that the results for the higher orders can be trusted. As shown in figures 7 (*b*), (*c*) and (*d*), normalized spectra of second, third and fourth order computed using the Gaussian formulation all lie rather remarkably close to the measured values of these spectra. The agreement becomes somewhat poorer as the order of the spectrum increases, and also noticeably degrades with increasing frequency for ϕ_3 and ϕ_4. One would expect the discrepancies between theoretical and experimental higher-order spectra to increase with increasing order, as the difference between the measured moments and those for a Gaussian random function increases as the order increases. The measured values of the first few higher-order moments for the mixing-layer data are $\langle u^3\rangle/\langle u^2\rangle^{\frac{3}{2}} = -0{\cdot}035$, $\langle u^4\rangle/\langle u^2\rangle^2 = 2{\cdot}6$, $\langle u^5\rangle/\langle u^2\rangle^{\frac{5}{2}} = -0{\cdot}16$, $\langle u^6\rangle/\langle u^2\rangle^3 = 10{\cdot}2$, $\langle u^7\rangle/\langle u^2\rangle^{\frac{7}{2}} = -0{\cdot}27$ and $\langle u^8\rangle/\langle u^2\rangle^4 = 52$, compared with corresponding Gaussian values of 0, 3, 0, 15, 0 and 105, respectively. The measured probability density, shown in figure 5, is quite symmetrical and to a low-order approximation is fairly well described by the Gaussian probability density.

In terms of an absolute-magnitude comparison like that made in §3 for the atmospheric inertial-subrange spectra, the unnormalized theoretical and measured values of ϕ_2 are in very good agreement, while in the low-frequency range, which produces the largest contributions to the moments, the theoretical and measured values of ϕ_3 and ϕ_4 are roughly in the ratios 3/2 and 2/1, respectively. This is the spectral equivalent of the difference between the directly measured higher-order moments and the corresponding Gaussian values. For these data then, the Gaussian assumption provides an accurate representation for third- and fourth-order spectra only in the normalized representation in which the total area under the spectral curves is equal to one.

5. Discussion and conclusions

The original Kolmogorov argument asserts that, if the energy spectrum ϕ_1 has a range in which it depends solely on ϵ and the wavenumber k, then it must have the form $\phi_1 = \alpha_1 \epsilon^{\frac{2}{3}} k^{-\frac{5}{3}}$ in that range. Dutton & Deaven proposed that, if the Kolmogorov argument could be extended in the sense that nth-order spectra ϕ_n also had a range in which they depended only on ϵ and k, then they must have the form given by (2). This expression is in serious conflict with the observations of Dutton & Deaven ($n \leqslant 4$) and the present data ($n \leqslant 9$). Hence we conclude that the Dutton & Deaven extension of the Kolmogorov argument is not valid. The present theoretical generalization (§2.1) of the Kolmogorov dimensional argument is based on the dissipation terms in the dynamical equations for $\langle u^{2n} \rangle$ and $\langle u^{2n+1} \rangle$. The resulting predicted variation of the higher-order spectra with wave-number is consistent with the experimental results. The Gaussian theory is also in good qualitative and quantitative agreement with the experiments.

The good agreement of the normalized mixing-layer spectral data with the Gaussian calculations shows that the Gaussian formulation can be used to predict accurately entire spectra of arbitrary order from the first-order spectrum or correlation function when the higher-order moments are known and the probability density is approximately Gaussian. Good absolute spectral agreement is obtained when the moments are close to those for a Gaussian distribution. Further measurements of this kind in other flows, especially a flow like grid turbulence, in which the probability density is more closely Gaussian, might serve as an interesting test of the order to which the Gaussian theory can furnish valid predictions for the ϕ_n.

We wish to thank Dr S. O. Rice, Dr K. N. Helland and Dr T. T. Yeh for much help with the analysis and computing done at UCSD, and Dr F. H. Champagne for kindly furnishing tabulated data for the BSRL plane-mixing-layer experiment. The research was supported by National Science Foundation Grant GK-43643X and the Advance Research Projects Agency of the Department of Defense and monitored by ONR under Contract N00014-69-A-0200-6054.

Appendix. Derivation of asymptotic form of the *n*th-order convolution of the von Kármán spectrum

Define $C_n(f)$ as the n-fold convolution of $(1+x^2)^{-\frac{5}{6}}$. The zeroth-order convolution is the spectrum itself, i.e. $C_0(f) = (1+f^2)^{-\frac{5}{6}}$. From Watson (1944, p. 185), the correlation function is

$$R(\tau) = \int_{-\infty}^{\infty} \frac{e^{-i2\pi\tau x}}{(1+x^2)^{\frac{5}{6}}}\, dx = \frac{2^{\frac{2}{3}}\Gamma(\frac{1}{2})}{\Gamma(\frac{5}{6})} |2\pi\tau|^{\frac{1}{3}} K_{\frac{1}{3}}(|2\pi\tau|), \tag{A 1}$$

where $K_{\frac{1}{3}}$ is the modified Bessel function of order $\frac{1}{3}$. Then

$$\begin{aligned} C_n(f) &= \int_{-\infty}^{\infty} e^{i2\pi f\tau}[R(\tau)]^{n+1}\, d\tau \\ &= c^{n+1}\frac{1}{\pi}\,\mathrm{Re}\int_0^{\infty} e^{izf}[z^{\frac{1}{3}}K_{\frac{1}{3}}(z)]^{n+1}\, dz, \end{aligned} \tag{A 2}$$

where $z = 2\pi\tau$ and $c = 2^{\frac{2}{3}}\pi^{\frac{1}{2}}/\Gamma(\frac{5}{6})$. From Watson (1944, p. 202), for large z

$$K_{\frac{1}{3}}(z) \sim (\pi/2z)^{\frac{1}{2}}\, e^{-z}(1 - 5/(72z) + \ldots). \tag{A 3}$$

Because of (A 3), the conditions for Jordan's lemma are satisfied, and we can swing the path of integration up along the imaginary z axis and, letting $z = iy$, we have

$$C_n(f) = \frac{c^{n+1}}{\pi}\,\mathrm{Re}\int_0^\infty i\,e^{-yf}[(iy)^{\frac{1}{3}}K_{\frac{1}{3}}(iy)]^{n+1}\,dy. \qquad \text{(A 4)}$$

Because of the exponential factor in the integrand, for large values of f the major contribution to the integral comes from small values of iy, and an asymptotic result for large f can be obtained by expanding the integrand for small values of $\xi = \frac{1}{2}iy$.

From the definition of $K_{\frac{1}{3}}$ (e.g. Watson 1944, pp. 77, 78)

$$z^{\frac{1}{3}}K_{\frac{1}{3}}(z) = \frac{\pi}{3^{\frac{1}{2}}}[z^{\frac{1}{3}}I_{-\frac{1}{3}}(z) - z^{\frac{1}{3}}I_{\frac{1}{3}}(z)].$$

Keeping the first few terms in the summations for $I_{\frac{1}{3}}$ and $I_{-\frac{1}{3}}$ and regrouping gives

$$z^{\frac{1}{3}}K_{\frac{1}{3}}(z) = b[1 - a\xi^{\frac{2}{3}} + \tfrac{3}{2}\xi^2 - \tfrac{3}{4}a\xi^{\frac{8}{3}} + \ldots]$$

and

$$\begin{aligned}[z^{\frac{1}{3}}K_{\frac{1}{3}}(z)]^{n+1} = d^{n+1}\Big[&1 - a(n+1)\xi^{\frac{2}{3}} + \tfrac{1}{2}n(n+1)\,a^2\xi^{\frac{4}{3}} \\ &+ \xi^2\left(\tfrac{3}{2}(n+1) - \frac{(n+1)\,n(n-1)}{3!}\,a^3\right) + \xi^{\frac{8}{3}} \\ &\times\Big(-\tfrac{3}{4}(n+1)\,a - \tfrac{3}{2}n(n+1)\,a \\ &\qquad + \frac{(n+1)\,n(n-1)(n-2)}{4!}\,a^4\Big) + \ldots\Big],\end{aligned} \qquad \text{(A 5)}$$

where $\xi = \frac{1}{2}iy$, $a = 3\Gamma(\frac{2}{3})/\Gamma(\frac{1}{3})$ and $d = 2^{\frac{1}{3}}\pi/3^{\frac{1}{2}}\Gamma(\frac{2}{3})$. From (A 4) and (A 5),

$$\begin{aligned}C_n(f) = [2\pi^{\frac{3}{2}}/3^{\frac{1}{2}}\Gamma(\tfrac{5}{6})\,\Gamma(\tfrac{2}{3})]^{n+1}\frac{3^{\frac{1}{2}}}{2\pi}\int_0^\infty dy\,e^{-yf}\,[a(n+1)\,(\tfrac{1}{2}y)^{\frac{2}{3}} - \tfrac{1}{2}n(n+1) \\ \times a^2(\tfrac{1}{2}y)^{\frac{4}{3}} - (\tfrac{1}{2}y)^{\frac{8}{3}}\,(\tfrac{3}{4}a(n+1)\,(2n+1) - \tfrac{1}{24}a^4(n+1)\,n(n-1)\,(n-2)) + \ldots].\end{aligned}$$

Integrating term by term yields an asymptotic series for large f:

$$\begin{aligned}C_n(f) \sim [\pi^{\frac{1}{2}}\Gamma(\tfrac{1}{3})/\Gamma(\tfrac{5}{6})]^n\,[(n+1)f^{-\frac{5}{3}} - 2^{-\frac{2}{3}}n(n+1)\,f^{-\frac{7}{3}} \\ + \tfrac{5}{6}\{-(2n+1) + \tfrac{1}{18}n(n-1)\,(n-2)\,a^3\}\,f^{-\frac{11}{3}} + \ldots],\end{aligned}$$

or

$$C_n(f) \sim (4{\cdot}20)^n\,[(n+1)f^{-\frac{5}{3}} - n(n+1)f^{-\frac{7}{3}}/1{\cdot}59 + \ldots].$$

REFERENCES

Brillinger, D. R. & Rosenblatt, M. 1967 Computation and interpretation of k-th order spectra. In *Spectral Analysis of Time Series* (ed. B. Harris), pp. 189–232. Wiley.

Champagne, F. H., Pao, Y. H. & Wygnanski, I. J. 1976 On the two-dimensional mixing region. *J. Fluid Mech.* (In press.)

Chen, W. Y. 1969 Spectral energy transfer and higher-order correlations in grid turbulence. Ph.D. thesis, University of California, San Diego.

Corrsin, S. C. 1951 On the spectrum of isotropic temperature fluctuations in an isotropic turbulence. *J. Appl. Phys.* **22**, 469.

Dutton, J. A. & Deaven, D. G. 1972 Some properties of atmospheric turbulence. In *Statistical Models and Turbulence. Lecture Notes in Physics*, vol. 12 (ed. M. Rosenblatt & C. W. Van Atta), pp. 402–426. Springer.

FRENKIEL, F. N. & KLEBANOFF, P. S. 1967 Higher-order correlations in a turbulent field. *Phys. Fluids*, **10**, 507–520.

HELLAND, K. N. 1974 Energy transfer in high Reynolds number turbulence. Ph.D. thesis, University of California, San Diego.

HINZE, J. O. 1959 *Turbulence.* McGraw-Hill.

KAIMAL, J. C., WYNGAARD, J. C., IZUMI, Y. & COTÉ, O. R. 1972 Spectral characteristics of surface layer turbulence. *Quart. J. Roy. Met. Soc.* **98**, 563–589.

KOLMOGOROV, A. N. 1941 The local structure of turbulence in an incompressible fluid for very large Reynolds numbers. *Dokl. Akad. Nauk S.S.S.R.* **30**, 301–305.

OBOUKHOV, A. M. 1941 On the distribution of energy in the spectrum of turbulent flow. *Dokl. Akad. Nauk S.S.S.R.* **32**, 19.

OBOUKHOV, A. M. 1962 Some specific features of atmospheric turbulence. *J. Fluid Mech.* **13**, 77–81.

RICE, S. O. 1973 Distortion produced by band limitation of an FM wave. *Bell Syst. Tech. J.* **52**, 605–626.

RICHARDSON, L. F. 1920 The supply of energy to and from atmospheric eddies. *Proc. Roy. Soc.* A **97**, 354.

TENNEKES, H. & LUMLEY, J. L. 1972 *A First Course in Turbulence.* M.I.T. Press.

TOWNSEND, A. A. 1947 The measurement of double and triple correlation derivatives in isotropic turbulence. *Proc. Camb. Phil. Soc.* **43**, 560–570.

VAN ATTA, C. W. 1974 Sampling techniques in turbulence measurements. *Ann. Rev. Fluid Mech.* **6**, 75–91.

VAN ATTA, C. W. & CHEN, W. Y. 1968 Correlation measurements in grid turbulence using digital harmonic analysis. *J. Fluid Mech.* **34**, 497–515.

VAN ATTA, C. W. & CHEN, W. Y. 1970 Structure functions of turbulence in the atmospheric boundary layer over the ocean. *J. Fluid Mech.* **44**, 145–160.

VAN ATTA, C. W. & PARK, J. 1972 Statistical self-similarity and inertial subrange turbulence. In *Statistical Models and Turbulence. Lecture Notes in Physics*, vol. 12 (ed. M. Rosenblatt & C. W. Van Atta), pp. 402–426. Springer.

WATSON, G. N. 1944 *Theory of Bessel Functions.* Cambridge University Press.

WYNGAARD, J. C. & PAO, Y. H. 1972 Some measurements of the fine structure of large Reynolds number turbulence. In *Statistical Models and Turbulence. Lecture Notes in Physics*, vol. 12 (ed. M. Rosenblatt & C. W. Van Atta), pp. 384–401. Springer.